Journal of Thermal Analysis, Vol. 44 (1995) 1417-1437

CONGRUENT MELTING OF BINARY COMPOUNDS WITH NON-NEGLIGIBLE VAPOUR PRESSURE
I. Theoretical aspects of the congruent melting of a hydrate

J.-C. Rouland[1], *A. Thorén*[2], *J.-L. Fournival*[3] *and R. Céolin*[3]

[1]Laboratoire de Chimie Physique, Faculté de Médecine et de Pharmacie, Place Saint-Jacques, F-25030 Besançon Cedex, France
[2]Laboratoire de Chimie Minérale, Faculté de Pharmacie, Avenue de l'Observatoire, F-75006 Paris, France
[3]Laboratoire de Chimie Physique, Faculté de Pharmacie, 2bis, Bd Tonnellé, F-37042, Tours Cedex, France

Abstract

A theoretical temperature–specific volume–molar fraction (T–v–x) phase diagram of the binary system $A - H_2O$ presenting a hydrate H with congruent melting is studied. The phase diagram is divided into two subsystems by the one-component phase diagram of the hydrate H. The eutectic invariant planes which occur in both subsystems are described. The relationships between the invariants are given.

Isochoric and isoplethal theoretical sections are given. The one-component phase diagram of the hydrate H is described. It is pointed out that the triple line solid–liquid–vapour which relates the congruent melting is not necessarily perpendicular to the molar fraction axis. The means that the three phases, solid, liquid and vapour, have not necessarily the same composition.

The T–v–x representation gives an explanation to the deviation between the maximum of the melting curve and the stoichiometric composition of the hydrate which is often observed in the T–x binary diagrams $A - H_2O$.

Keywords: congruent melting

Introduction

This paper deals with the theoretical approach we adopted in a project aimed at the study of systems with non-negligible pressure [1]. Such systems are usually studied by means of differential thermal analysis (DTA), using tubes sealed under vacuum. In earlier publications, we showed that the DTA results obtained under these conditions might well be interpreted in the three-dimensional T–v–x diagram, with temperature (T), specific volume (v) and molar fraction (x) as variables. The specific volume v is equal to the ratio V/m, where V is the internal volume of the tube and m is the total mass of the sample.

0368–4466/95/ $ 4.00

John Wiley & Sons, Limited
Chichester

We earlier studied two series of binary systems. The systems of the first series were based on arsenic, and the systems of the second series on water. The binary compounds were neodymium diarsenide, $NdAs_2$ [2], phenobarbital hydrate and *L*-citrulline hydrate [3, 4]. Each of these binary compounds showed an incongruent melting point in the presence of a vapour phase. Hence, four phases were present at peritectic equilibrium: two solid phases, one liquid phase and one vapour phase. Each of the four phases in equilibrium is characterized by its own composition and its own specific volume. Furthermore, on each isochoric section, at the peritectic invariant, the position of the binary compound deviates from the stoichiometric composition. The composition of the point representing the binary compound at the peritectic invariant is richer in the more volatile constituent. This deviation becomes more important when the specific volume increases and when the difference between the vapour pressure of the two constituents increases.

By means of DTA in sealed tubes, we also studied binary compounds which exhibit congruent melting: sulfaguanidine hydrate and 1,10-phenanthroline hydrate [5, 6]. In these cases, three phases (solid, liquid and vapour) were also in equilibrium at the melting point, and we observed again that the compositions of these three phases were different. At first sight, this seems to be inconsistent with the usual definition of congruent melting.

However, this phenomenon has also been observed by Tmar *et al.* [7], who indicated that gallium arsenide (GaAs) presented a congruent melting point in the presence of a vapour phase, and observed that the vapour phase contained much more arsenic than gallium.

Elsewhere, Zernicke [8] stated that, for binary compounds, the maximum in the melting curve does not necessarily occur at the stoichiometric composition. This phenomenon is generally explained by the presence of a solid solution. However, the existence of a solid solution does not usually involve any modification of the melting process. The melting may be congruent with or without the existence of a solid solution: the solid and liquid phases which coexist at the melting point have the same composition, that of the initial solid sample. This implies that, in a closed vessel, the vapour, the liquid and the solid phases in equilibrium with one another have the same composition.

The phenomenon which we have observed for hydrates is different. The deviation between the maximum in the melting curve and the stoichiometric composition of the hydrate is not the only observed phenomenon. We have also observed that the compositions of the three phases at equilibrium are not the same. The vapour phase contains more water (the more volatile constituent) than the initial sample. Thus, at least one of the two remaining phases has also changed.

This cannot be explained by the presence of a solid solution. Accordingly, we used the temperature-specific volume–molar fraction (T–v–x) representation to interpret these systems.

When DTA is performed with sealed tubes, the analysis conditions are not isobaric, but isochoric. However, this method does not allow the dead volume of the tube to be eliminated. On heating, a saturating vapour phase fills up this dead volume. If the vapour pressure is sufficiently low to be neglected, the binary system may be interpreted as an isobaric system, i.e. by an isobaric *T–x* diagram. If the vapour pressure is not negligible, the dead volume must be eliminated experimentally. In this case, the phase changes will be observed only if the vessel dilates to the same degree as the sample.

It is not easy to achieve this kind of experiment. Hence, instead of trying to eliminate the dead volume, we decided to make it vary and to monitor its variations. The DTA results were then reported in a *T–v–x* diagram.

Representation in a *T–v–x* diagram of the three phases (solid, liquid and vapour) at the triple point, for a hydrate *H*

First, the three phases at the melting equilibrium must be located in the *T–v–x* diagram. The corresponding specific volumes and molar fractions will then be known.

If this melting is regarded as classical melting, the solid and liquid phases must have the same composition. As mentioned above, the vapour phase is found to be much richer in water than the other two phases (solid and liquid). Hence, in the *T–v–x* plane, the melting equilibrium must be represented by a triangle (Fig. 1) and, in each isochoric section, the congruent melting must be described as a horizontal segment *MN* (Fig. 2-A). However, such a segment relates the existence of a peritectic invarient. Thus, this interpretation cannot be correct.

In an isochoric section, the correct representation of a congruent melting is one point: point *N* in Fig. 2-B. However, the compositions of the three phases at equilibrium are not necessarily equal. Consequently, the only correct representation of the congruent melting of a hydrate is the segment *S–L'–V* in Fig. 1, which connects the three points representing the solid, liquid and vapour phases at the melting equilibrium. This means that, in an isochoric section, for a given value of the specific volume, congruent melting will be observed for a sample whose initial composition is necessarily different from the stoichiometry of the hydrate.

Description of a binary system *A* – H_2O with a hydrate H in the *T–v–x* space

In this section, we deal with the theoretical diagram of a system *A* – H_2O presenting one monohydrate with congruent melting. This hydrate divides the system into two subsystems. In each subsystem, a eutectic invariant exists.

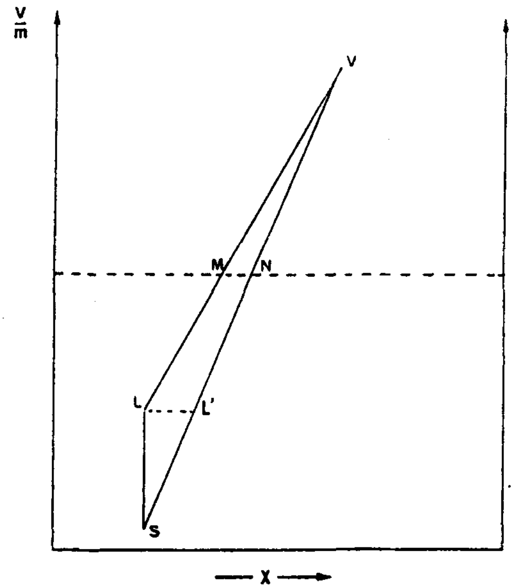

Fig. 1 Graphic representation of the solid (*S*), liquid (*L*) and vapour (*V*) phases, at the melting equilibrium of a hydrate, in the *T–v–x* plane.
Hypothesis 1: the compositions of the solid *S* and liquid *L* are equal; the vapour *V* is richer in more volatile constituent.
Hypothesis 2: the compositions of the solid *S* and the liquid *L'* are different; *S, L'* and *V* are aligned

We do not assume any hypothesis about the molecular nature of the vapour, and our demonstration is based on conclusions presented in previous papers:

– in *T–v–x* diagrams, invariant equilibria are represented by four-phase reactions,

– each phase is characterized by its own specific volume,

– the invariant plane is either a quadrilateral or a triangle with a central phase [1],

– the specific volume of vapour a phase is always higher than the specific volumes of the condensed phases in equilibrium.

As concerns the particular case of the systems *A* – H_2O, we assume that the anhydrous compound *A* is much less volatile than water. This implies that the vapour phase is much richer in water than the condensed phases in equilibrium.

The eutectic invariant of the *A* side of the diagram is triangular since the specific volume of the liquid *A* is presumed to be higher than that of the solid *A*. In contrast, the specific volume of liquid water is smaller than that of ice. This implies that the eutectic invariant between hydrate and water is quadrilateral. This is the particular case for the systems *A* – H_2O. In the general case, eutectic planes are triangular.

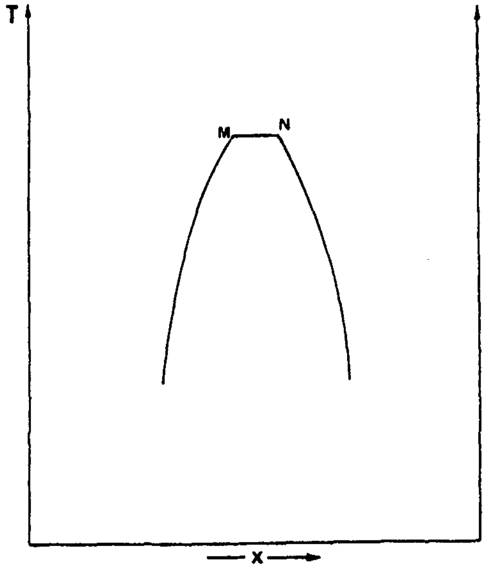

Fig. 2A Representation of the congruent melting of a hydrate in the *T*–*x* plane (hypothesis 1)

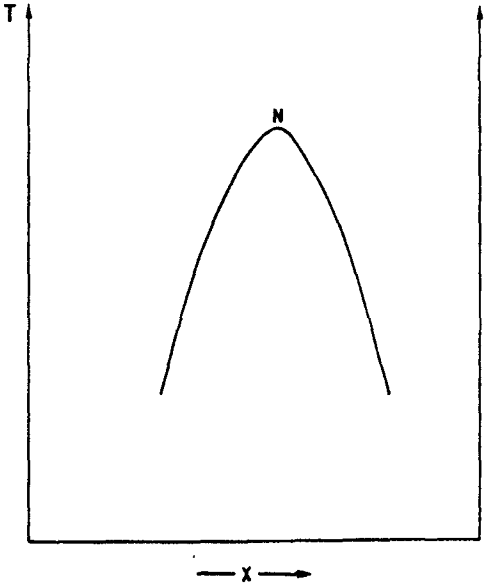

Fig. 2B Representation of the congruent melting of a hydrate in the *T*–*x* plane (hypothesis 2)

Description of the invariants

Figure 3 shows the projection of the two eutectic invariants on the v–x plane. The anhydrous-side invariant plane is found to be triangular. It relates a four-phase equilibrium between anhydrous form (A), hydrate (H), eutectic liquid (e_1) and vapour phase (G_1^0):

$$A + H + \text{vapour } G_1^0 \rightleftharpoons \text{liquid } e_1$$

The forward reaction takes place when the temperature rises.

The water-side invariant plane is quadrilateral. It relates a four-phase equilibrium between hydrate (H), ice (S_{H_2O}), eutectic liquid (e_2) and vapour phase (G_2^0):

$$H + \text{ice} \rightleftharpoons \text{liquid } e_2 + \text{vapour } G_2^0$$

The forward reaction takes place when the temperature rises.

In Fig. 3, the temperature T_1 of the eutectic point e_1 is higher than the temperature T_2 of the eutectic point e_2. T_2 is close to 0°C and the points representing the vapour, G_1^0 and G_2^0, have different V/m values.

Experimental data obtained on other systems [2] show that the compositions of the water-rich vapour phases G_1^0 and G_2^0 are not very different. Since the specific volume increases when the temperature decreases, as shown in the P–T–v diagrams of the pure compounds, it is likely that, in most cases, the specific volume of G_2^0 will be greater than that of G_1^0. This is indicated in Fig. 3.

Relationship between the invariants

As usual, the binary compound H divides the system into two subsystems, $A - H$ and H–H_2O. Furthermore, the existence of a third dimension, v, and the presence of a vapour phase in equilibrium with the hydrate H, implies that the limit between the two subsystems is not a segment perpendicular to the molar fraction axis, but a figure which represents the phase diagram T–V/m of pure hydrate H. The values of the specific volumes and compositions of the liquid and solid phases in equilibrium with one another determine the inclination of this one-component phase diagram in relation to the x-axis.

In the classical isobaric T–x representation, the liquidus curve on each side of the solid binary compound falls from the melting point. In the T–v–x representation, the ruled surfaces, which limit the three three-phase solid-liquid-vapour regions, fall in the same way from the triple line H–L–G (Fig. 4). These vaporus surfaces form two solid–liquid–vapour regions above the invariant planes. Figure 3 shows that the bases of these two regions are the triangles

H–e_2–G_1° (at the temperature of the eutectic e_1) and H–e_2–G_2° (at the temperature of the eutectic e_2).

The triple line H–L–G is orthogonal to the temperature axis. It relates the melting of the hydrate H. The points H, L and G represent the solid, liquid and vapour phases at the melting equilibrium. They are necessarily aligned; if they were not, the melting would not be congruent: there would be a fourth phase, which would make the invariant plane quadrilateral.

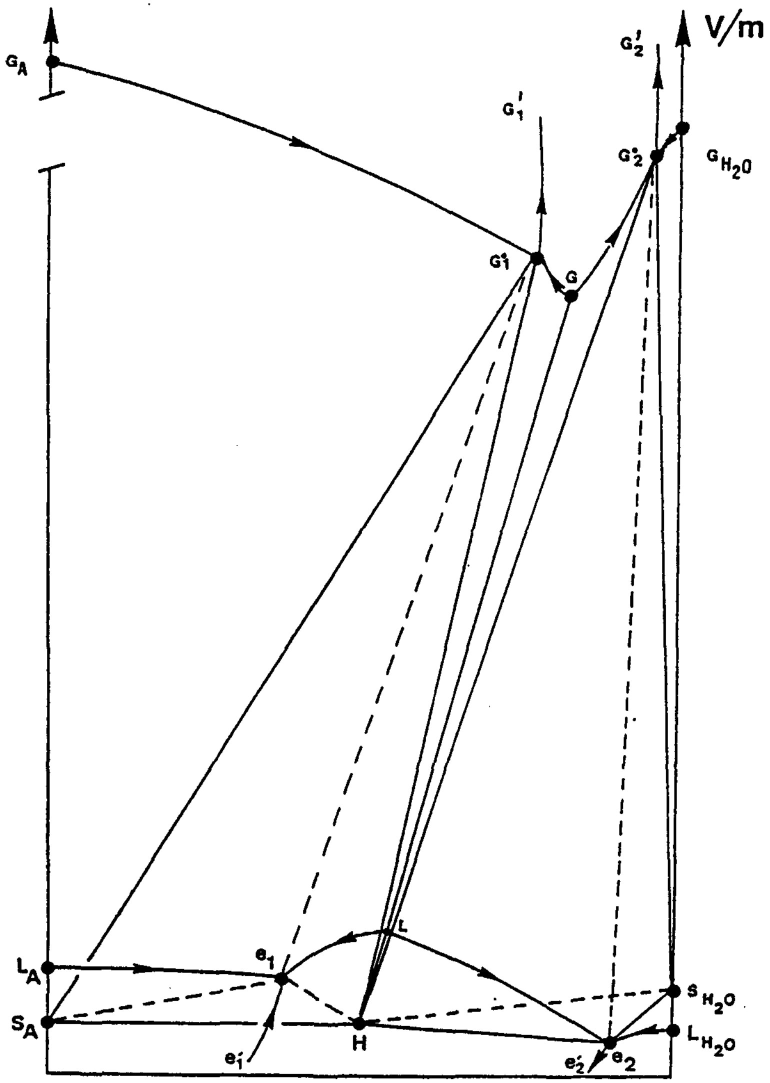

Fig. 3 Projection of the eutectic invariant planes and liquidus and vaporus valleys in the x–V/m plane

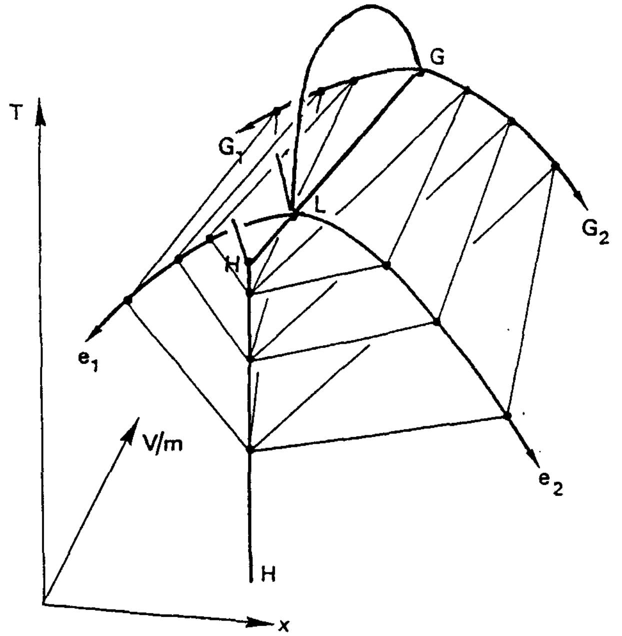

Fig. 4 Representation of the ruled surfaces limiting the three-phase regions solid hydrate (H)–liquid(L)–vapour(G)

The segment H–S–G may be called a triple line. This is consistent with the representation of the melting of a pure substance in a closed vessel, which is described by a triple line in the T–v diagram. In the same way, the melting of a pure binary compound must be represented by a triple line in the T–v–x binary diagram.

However, it must be pointed out that the triple line of the T–v–x diagram is not necessarily perpendicular to the x-axis since solid, liquid and vapour phases do not necessarily have the same composition. In the present case of a system A – H_2O, the triple line will not be perpendicular to the x-axis.

Delimitation of the regions

Three valleys converge to the points which represent the liquid and the vapour phases in equilibrium with one another at the eutectic temperature, exactly as may be observed at the eutectic, in isobaric diagrams of ternary systems.

The liquidus and vaporus valleys which converge to the points e_1, e_2, G_1 and G_2 are shown in Fig. 3. Since the pressure of the vapour in equilibrium with the anhydrous solid at the triple point is low, the point which represents the vapour phase corresponds to a very high specific volume.

Figure 5 presents a perspective diagram of the liquidus and vaporus valleys. The curve $S'(A)$–$S(A)$–$S''(A)$ corresponds to the solidus curve of the anhydrous compound *A*. To keep the Figure clear, the other solidus curves are not represented. This Figure also shows the two-phase region (liquid–vapour) which is limited in its upper part by the critical line (*C*). This critical line joins the critical points of the liquid–vapour region of the pure constituents (*A* and water).

Most of the regions of this diagram are similar to those described in our previous study of the incongruent melting of the binary compound $NdAs_2$. In the present study, we describe only the regions which are particular to the *A* – H_2O diagram, and especially the regions containing water. As a matter of fact,the general shape of this diagram is quite original in the region of low specific volumes, since the specific volume of ice is greater than that of liquid water.

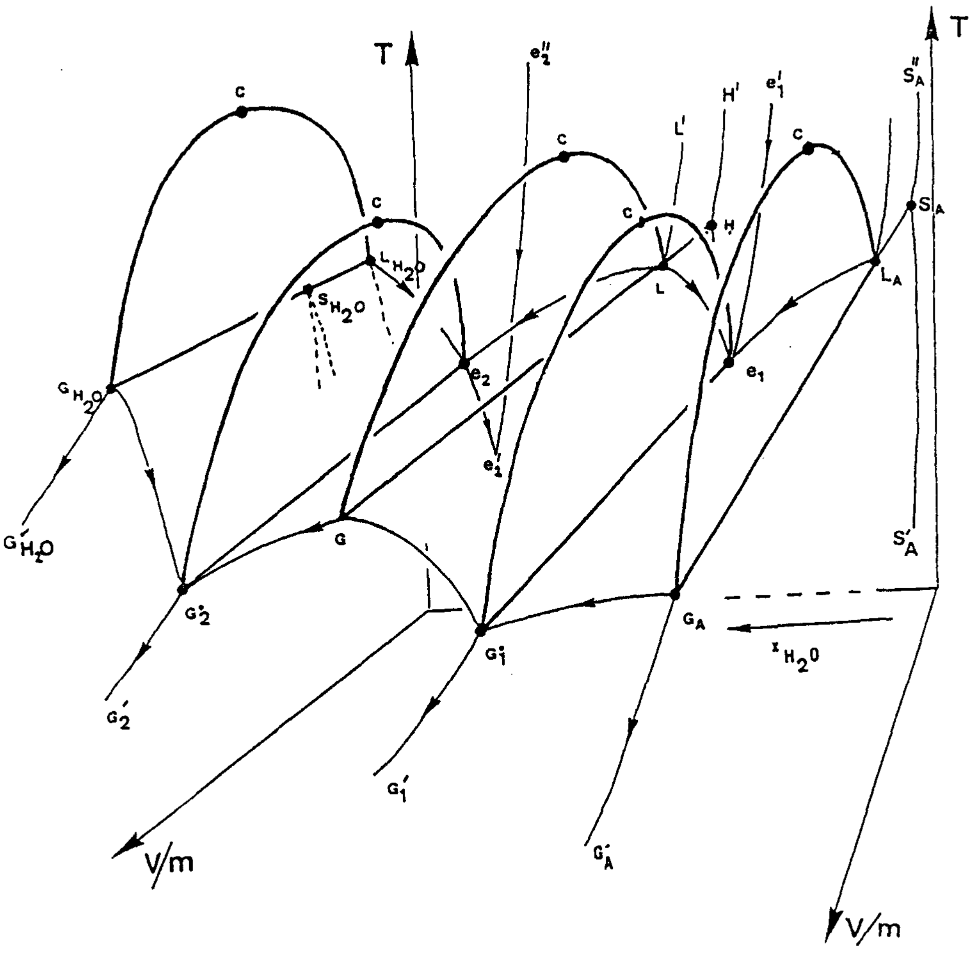

Fig. 5 Representation of the different liquidus and vaporus valleys in the *T*–*v*–*x* diagram

Description of one-phase regions (liquid or vapour)

Figure 6 shows the projection of the vaporus and liquidus surfaces on the x–V/m plane. The critical line obtained with points C marks the continuity between liquid and vapour states. This Figure is graduated with an arbitrary temperature scale. It shows another critical line, which is formed by the series of points C'. We found no reason for the projections of points C' to be aligned with H–L–G. Hence, the scheme of Fig. 6 represents merely a special case. In con-

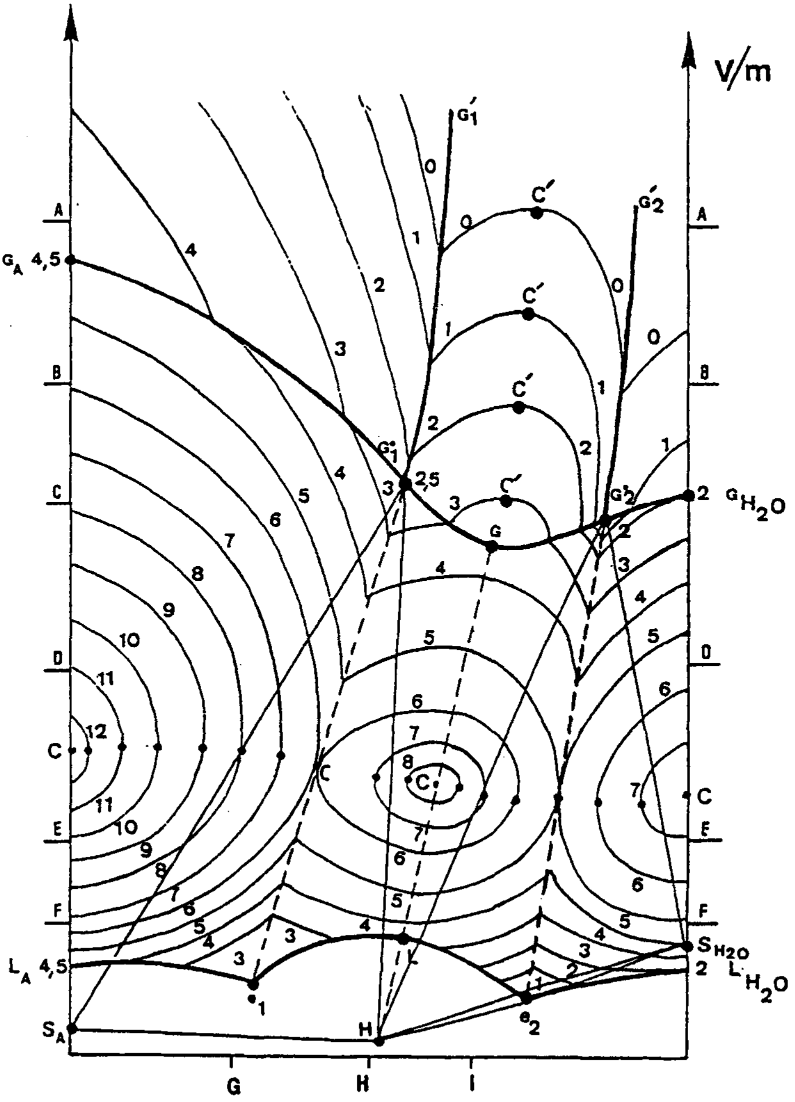

Fig. 6 Projection of the vapours and liquidus surfaces in the plane x–V/m

trast, curve (C') starting from point G and going to the higher V/m values must not intercept either the vapour valley G_1^o–G'_1, or G_2^o–G'_2.

Description of water-rich regions

Figure 7 shows the T–v diagram of pure water, drawn from the P–T–v diagram by Bruhat [9]. This diagram shows the existence of six crystalline forms of ice. These different forms are responsible for the existence of several invariant planes in the three-dimensional T–v–x diagram of the systems A – H_2O.

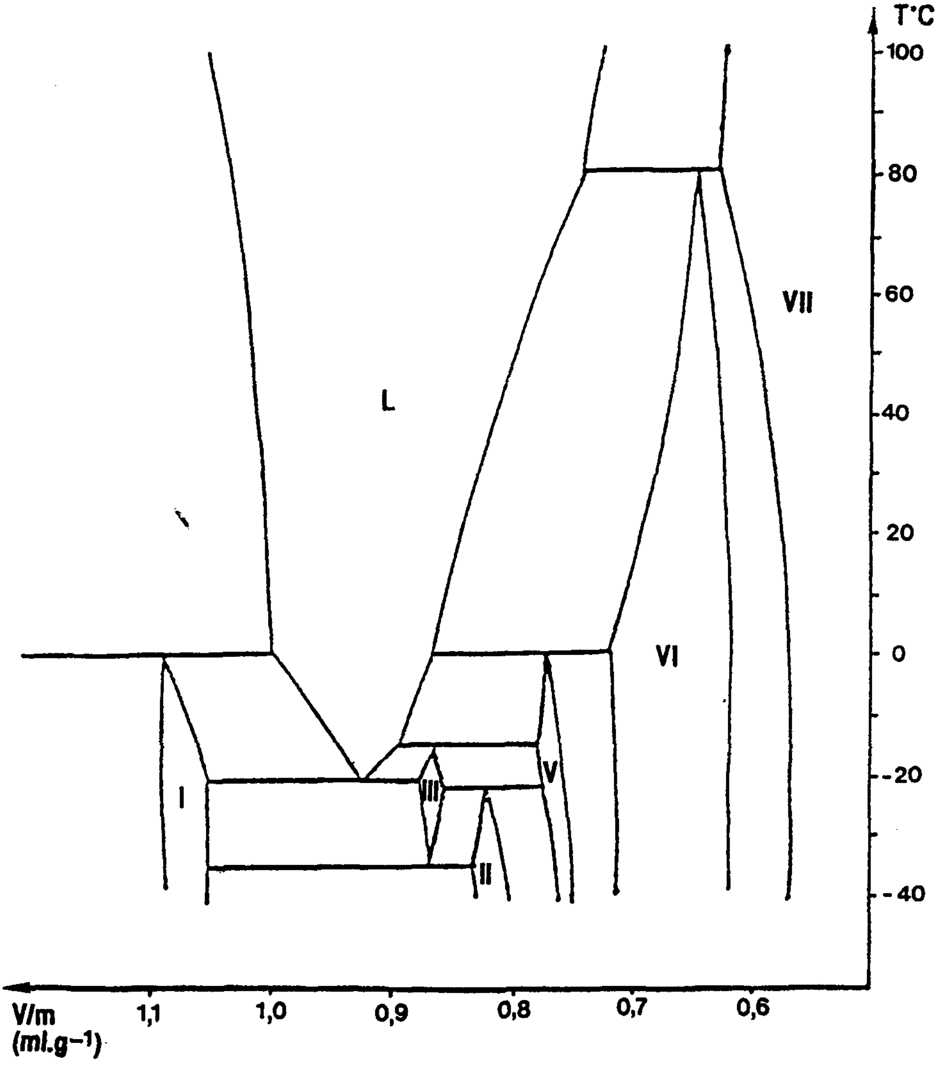

Fig. 7 T–v–m phase diagram of water

Figure 8 shows two of these invariant planes. The Figure has been simplified by stating arbitrarily that there is no solid solution around forms I and II of ice.

Only one of these two planes, plane P_2, can be observed below 0°C for the *V/m* values which can be obtained experimentally. This plane is a quadrilateral eutectic plane where the following equilibrium exists:

$$\text{hydrate } H + \text{ice (form I)} \rightleftharpoons \text{liquid } e_2 + \text{vapour } G_2^{\circ}$$

Two liquidus valleys converge to point e_2. They fall from point L (liquid phase at the triple line of the hydrate phase diagram) and from point LH_2O (liquid phase at the triple line of the water phase diagram). From point e_2, a third liquidus curve falls to plane P'_2. This last invariant plane lies between forms I and III of ice and the hydrate. It relates the following equilibrium:

$$\text{ice I} + \text{ice III} + \text{hydrate } H \rightleftharpoons \text{liquid } e'_2$$

Two other liquidus curves converge to e'_2. One comes from point e_{H_2O} of the water phase diagram, while the other comes from a quadrilateral invarint plane where forms III and V of ice and the hydrate form interact.

The only regions which will be described here are those where form I of ice is present, since it is the only form which is in stable equilibrium with the vapour phase (Figs 3, 5 and 8).

Two-phase region (ice+vapour) (Figs 3 and 5)

This region is limited by the vapour surface $G'_{H_2O}-G_{H_2O}-G_2^{\circ}-G'_2$ and the two ruled surfaces which spread out between the solidus S_{H_2O} and the vaporus curves $G_{H_2O}-G_2^{\circ}$ and $G_2^{\circ}-G_2'$.

Three-phase region (ice+liquid+hydrate) (Fig. 5)

This region is limited by the ruled surface which forms between the solidus of hydrate H and the liquidus curve $e_2-e'_2$. The liquidus curve falls from e_2 to e'_2. Thus, this region is present at temperatures lower than that of the invariant plane $H-e_2-S_{H_2O}-G_2^{\circ}$.

Three-phase region (ice-liquid-vapour) (Figs 3 and 5)

This region is limited by the rule surface which forms between the vapours curve $G_{H_2O}-G_2^{\circ}$, the solidus curve S_{H_2O} and the liquidus curve $L_{H_2O}-e_2$. It extends from the triangle $S_{H_2O}-e_2-G_2^{\circ}$ (on the invariant plane P_2) to the triple line of pure water $L_{H_2O}-S_{H_2O}-G_{H_2O}$.

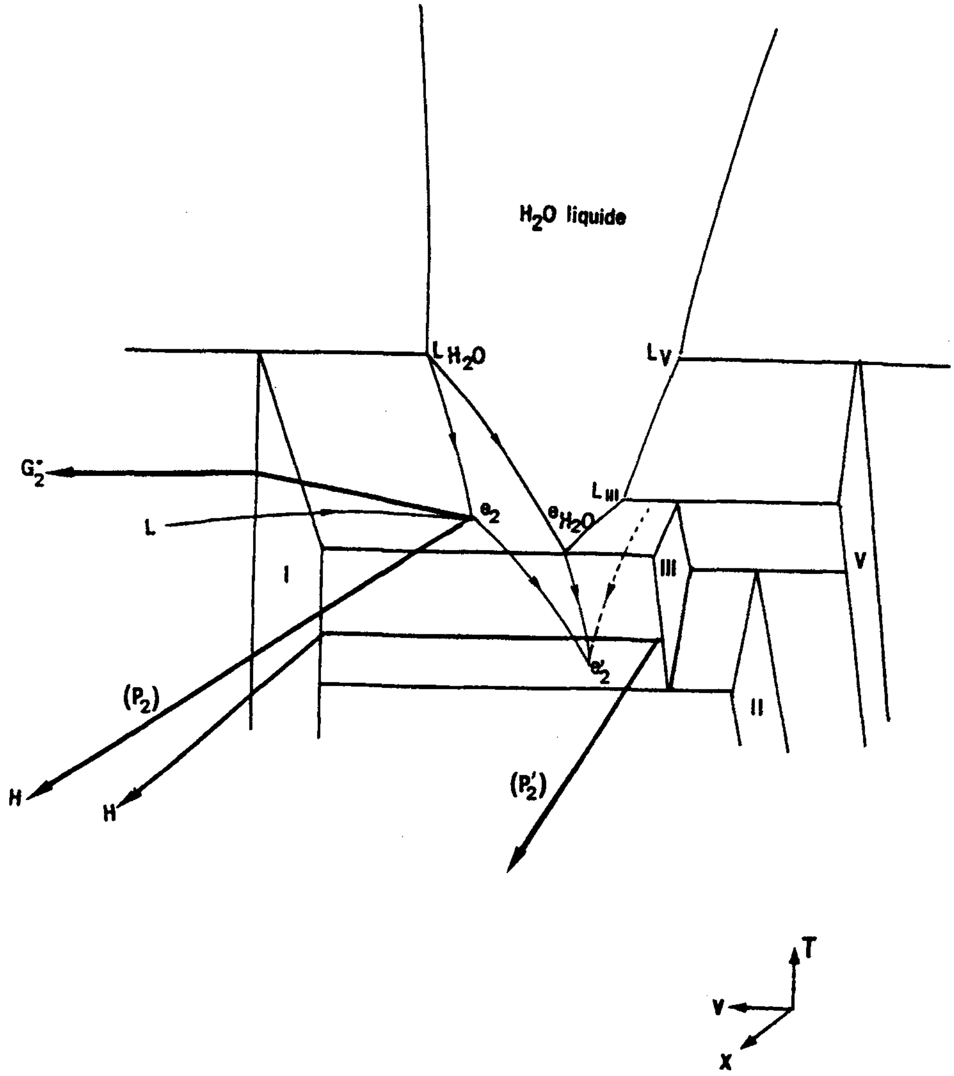

Fig. 8 Representation of the invariant planes (P_2) and (P_2') where forms I and III of ice interact. The liquidus curves which fall to the points e_2 and e_2' originate at the T–V/m diagram of water. The dotted lined liquidus curve passes through two invariant planes which are not represented in this figure and which relate equilibria where forms III and V of ice take place

Three-phase region (ice–hydrate–vapour) (Figs 3 and 5)

This region is limited by the three ruled surfaces which form between the vaporus curve G_2^0–G_2', and solidus of the hydrate H and ice S_{H_2O}.

Two-phase region (ice–liquid) (Fig. 8)

This region spreads between the liquidus surface limited by the four liquidus curves $L_{H_2O}-e_{H_2O}$, $e_{H_2O}-e'_2$, $L_{H_2O}-e_2$ and $e_2-e'_2$ and the ruled surfaces coming from form I of ice and ending on the four liquidus curves.

Description of the regions involved by the congruent melting of the hydrate *H*

Two-phase region (solid hydrate–vapour) (Figs 3, 5 and 9)

This region is limited by the ruled surfaces coming from the solidus of the hydrate *H* which leans on the vaporus curves G–G_1°, G–G_2°, $G_1^\circ-G'_1$ and $G_2^\circ-G'_2$,

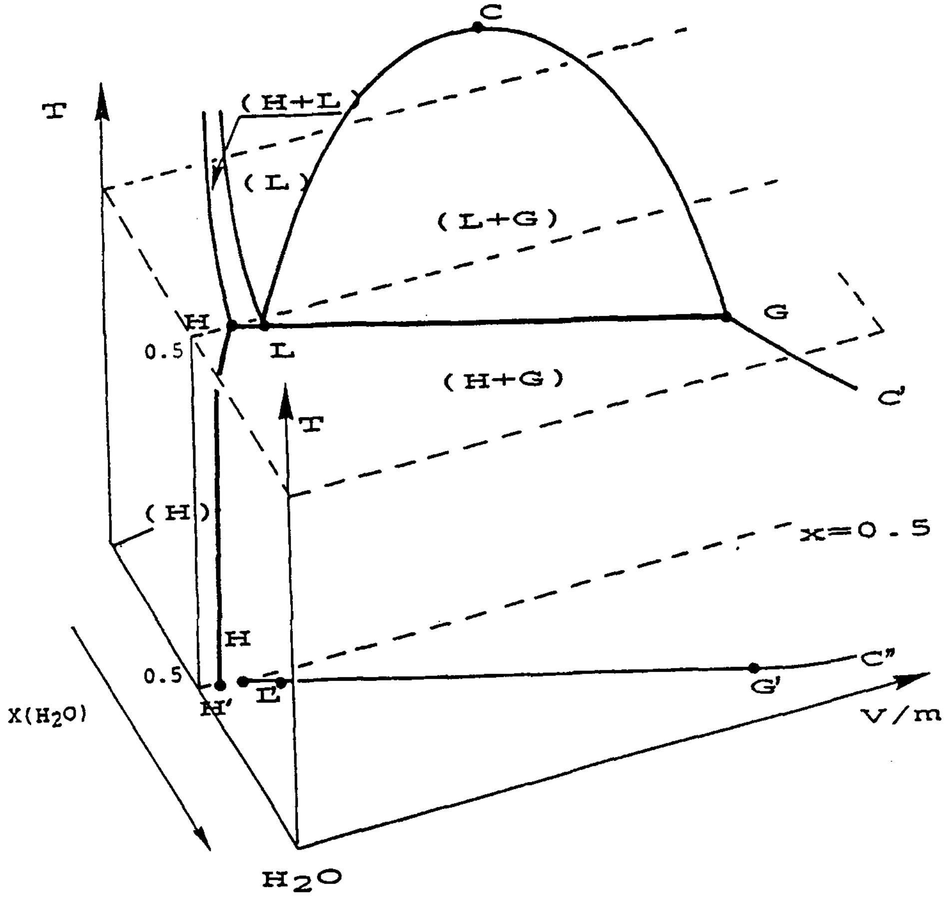

Fig. 9 Phase diagram of the congruent melting hydrate in the *T–V/m–x* space and projection of the triple line *H-L-G* on the plane *V/m–x*

and by the vaporus surface formed by these four curves. It is limited, at higher temperatures, by the triple line *H–L–G*. When an isochoric diagram is drawn, pure hydrate does not appear at the stoichiometric composition, as it does on the isobaric diagrams *T–x* but it appears in this two-phase region (solid–vapour).

T–v phase diagram of the hydrate form

Figure 9 shows that the section which divides the *T–v–x* diagram into two parts (that of the eutectic e_1 and that of the eutectic e_2) must be regarded as the phase diagram of the pure hydrate *H*. If, as indicated, points *H*, *L* and *G* are aligned, it is possible to draw a one-constituent diagram where the usual phase regions of one-component systems appear. This diagram is the *T–v* phase diagram of hydrate *H*. However, it is not entirely planar. As shown above, curve *GC'* is not necessarily in the plane formed by the triple line *H–L–G*, the curve *L–C–G* and the solidus *H–H'* of hydrate *H*. Consequently, the surface (*H*+*G*) is not a plane. It corresponds to a ruled surface the limits of which are the solidus of the hydrate *H–H'* and the vaporus curve *GC'*.

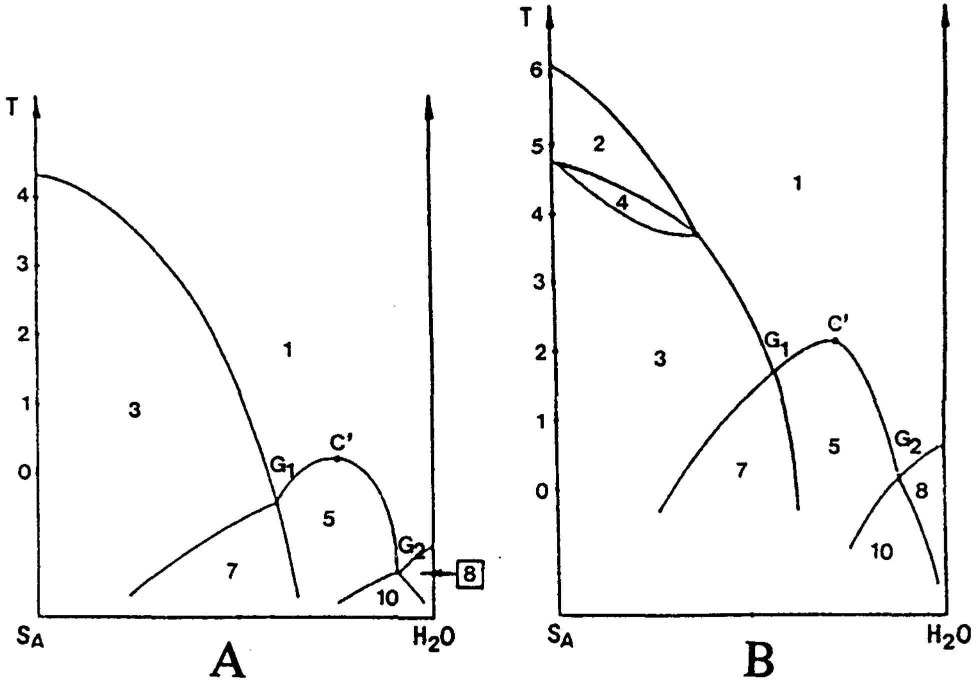

Fig. 10 Isochoric sections of the *T–V/m–x* diagram. The labels A to F of the sections are those of Fig. 6

Isochoric section

Three kinds of section can be drawn in the T–v–x diagram: isochoric, isothermal and isoplethal sections.

The isochoric sections are the most significant because they correspond to the experimental diagrams obtained by analysing samples of constant, or nearly constant, specific volumes.

Figures 10 to 12 represent isochoric sections (A to F). They show the variation in the liquidus curves and the variation in the areas of the different regions as functions of v. If these diagrams were interpreted as isobaric diagrams, the existence of solid solutions could be assumed.

The temperature scale is the same as the arbitrary scale used in Fig. 6. In sections A and B, points G_1 and G_2 represent the traces of the vaporus valleys G_1–G'_2 and G_2–G'_2, respectively. Point C' represents the trace of the critical line GC' of Fig. 6.

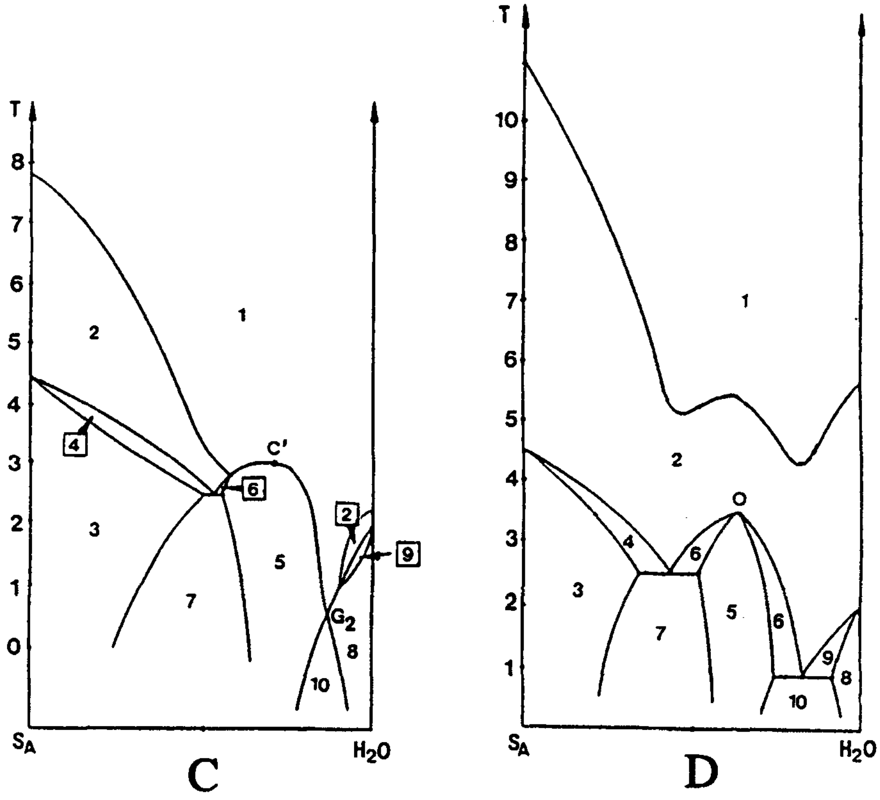

Fig. 11 Isochoric section of the T–V/m–x diagram. The labels A to F of the sections are those of Fig. 6

At the highest v values (section *A*), the only equilibria which occur are of the solid–vapour kind. In this section, the two-phase region (hydrate+vapour) can be observed (region 5). This region corresponds to the sublimation of the hydrate.

In sections *C* to *E*, the invariant eutectic between the anhydrous solid *S*(*A*) and hydrate *H* appears. In sections *D* to *F*, two three-phase regions (hydrate–liquid–vapour) (regions 6) lie above region 5. They converge to point *O*. Point *O* corresponds to the trace of the triple line *H–L–G* of the hydrate (Figs 3 and 6).

The limits between regions 6 and 2 are observed at temperatures below that of point *O* and at compositions ranging on both sides of the composition of point *O*. This corresponds to congruent melting of the hydrate.

In sections *D*, *E* and *F*, congruent melting of hydrate *H* is observed at water-rich compositions ($xH_2O>0.5$). The temperature of point *O* (congruent melting of the hydrate) is constant when v decrease. The trace of the invariants becomes larger and regions 5, 3 and 8 become smaller.

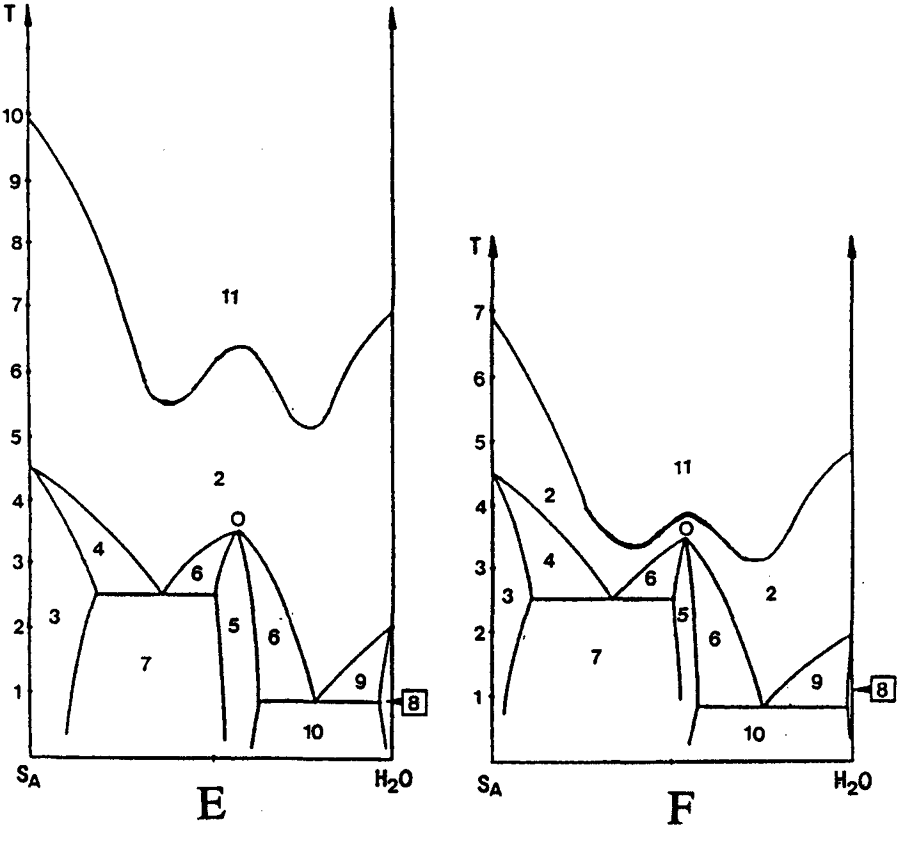

Fig. 12 Isochoric sections of the *T–V/m–x* diagram. The labels *A* to *F* of the sections are those of Fig. 6

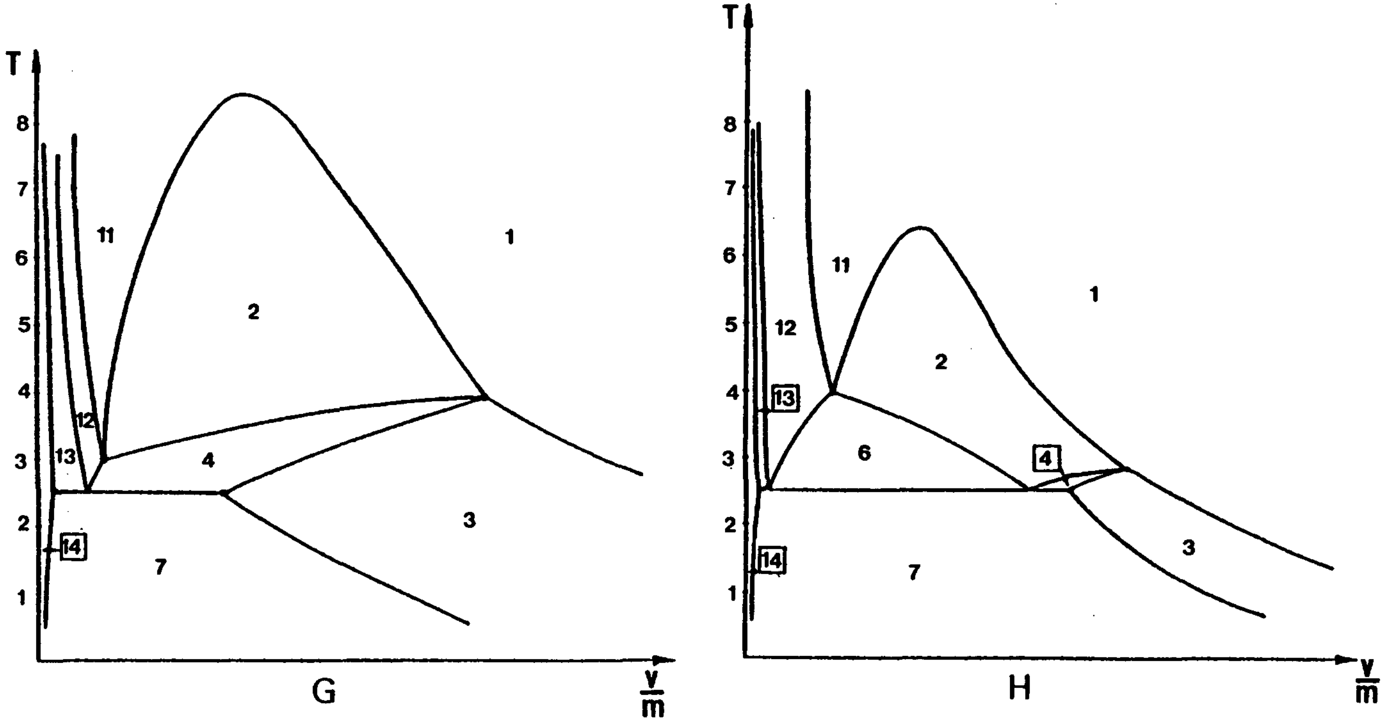

Fig. 13 Isoplethal section of the T–v–x diagram. The labels *G* to *I* of the sections are those of Fig. 6

Table 1 Number indicating the different phases present in the isochoric and iso-plethal sections:

1: vapour
2: liquid +vapour
3: anhydrous solid S_A +vapour
4: anhydrous solid S_A +liquid +vapour
5: hydrate H +vapour
6: hydrate H +liquid +vapour
7: anhydrous solid S_A +hydrate H+vapour
8: ice S_{H_2O} +vapour
9: ice S_{H_2O} +liquid +vapour
10: ice S_{H_2O} +hydrate H +vapour
11: liquid
12: anhydrous solid S_A +liquid
13: anhydrous solid S_A +hydrate H +liquid
14: anhydrous solid S_A +hydrate H
15: hydrate H +liquid
16: ice S_{H_2O} +hydrate H +liquid

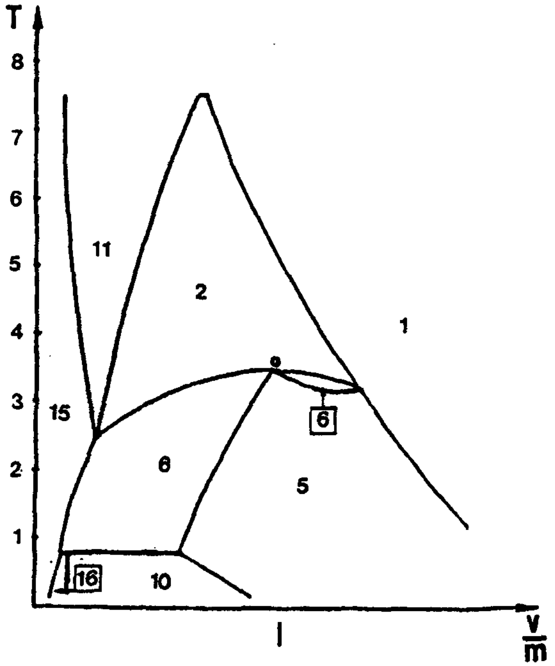

Fig. 14 Isoplethal sections of the T–v–x diagram. The labels G to I of the sections are those of Fig. 6

Isoplethal sections

Figures 13 and 14 represent three isoplethal sections (*G, H* and *I*) which correspond to the same temperature scale as that in Fig. 6. Point *O* is the trace of the triple line *H–L–G* of the hydrate. The presence of this point is due to the congruency of the melting.

Conclusions

In this study, we have drawn the theoretical *T–v–x* diagram of a binary system $A - H_2O$ presenting a hydrate form *H* with congruent melting. The system is divided into two subsystems by the phase diagram of hydrate *H*. It can be assessed that this diagram is not necessarily a plane. Furthermore, if compound *A* is much less volatile than water, the triple line solid–liquid–vapour of *H* is not perpendicular to the molar fraction axis. This gives the explanation of the deviation generally observed between the maximum in the melting curve and the stoichiometric composition of hydrates, when samples are analysed in closed vessels. The explanation of this deviation does not require the existence of a solid solution. From this *T–v–x* diagram, it is also clear that the three phases in equilibrium at the triple line do not have the same composition.

In our next paper, this theoretical diagram will be applied to the sulfaguanidine–water system, where sulfaguanidine monohydrate is found. We can assume that this theoretical diagram may also be used to interpret other kinds of systems with non-negligible vapour pressure, where a binary compound is present, especially mineral systems.

References

1 J. C. Rouland, C. Souleau and R. Céolin, J. Thermal Anal., 30 (1985) 429; 1081.
2 J. C. Rouland, R. Céolin and C. Souleau, J. Thermal Anal., 31 (1986) 305.
3 J. L. Fournival, J. C. Rouland and R. Céolin, J. Thermal Anal., 34 (1988) 161.
4 J. L. Fournival, R. Céolin, J. C. Rouland, P. Toffoli, P. Khodadad and J. Astoin, J. Thermal Anal., 32 (1987) 213.
5 G. Thévenet, Thesis University Paris-Sud, 1980.
6 J. L. Fournival, Thesis University Paris-Sud 1987.
7 M. Tmar, A. Gabriel, C. Chatillon and I. Ansara, J. Crystal Growth, 69 (1984) 421.
8 J. Zernicke, 'Chemical Phase Theory', Kluwer's Publishing Co. Ltd, Deventer, Pays-Bas, 1955.
9 G. Bruhat, 'Thermodynamique', 6e édition, Masson, Paris 1968, p. 319.

Zusammenfassung — Es wurde ein theoretisches Temperatur-Spezifisches Volumen-Molenbruch (*T-v-x*) Phasendiagramm des binären Systemes $A - H_2O$ untersucht, welches ein kongruent schmelzendes Hydrat *H* aufweist. Das Phasendiagramm wird durch das Einkomponenten-Phasendiagramm des Hydrates *H* in zwei Subsysteme unterteilt. Die in beiden Subsystemen vorkommenden eutektischen invarianten Ebenen werden beschrieben. Die Beziehung zwischen den Invarianten wird gegeben.

Es werden isochore und isoplethale theoretische Abschnitte gegeben. Das Phasendiagramm des Einkomponentensystems des Hydrates *H* wird beschrieben. Es wird gezeigt, daß die dem kongruenten Schmelzen zugehörende Tripellinie nicht unbedingt senkrecht zur Molenbruchachse steht. Dies bedeutet, daß die drei Phasen (feste, flüssige, gasförmige) nicht unbedingt die gleiche Zusammensetzung haben.

Die T-v-x -Darstellung liefert eine Erklärung zur Abweichung zwischen dem Maximum der Schmelzkurve und der stöchiometrischen Zusammensetzung des Hydrates, wie sie in binären T-x -Diagrammen von $A - H_2O$ Systemen oft beobachtet wird.